

MEASUREMENT OF RADICAL-SPECIES CONCENTRATIONS  
AND POLYCYCLIC AROMATIC HYDROCARBONS  
IN FLAMES BY FLUORESCENCE AND ABSORPTION  
USING A TUNABLE DYE LASER

MASTER

Progress Report  
March 1, 1980 - February 28, 1981

Robert P. Lucht  
Donald W. Sweeney  
Normand M. Laurendeau

The Combustion Laboratory  
School of Mechanical Engineering  
Purdue University  
West Lafayette, Indiana 47907

March, 1981

Prepared for

THE UNITED STATES DEPARTMENT OF ENERGY  
UNDER CONTRACT NO. DE-AS02-78ER04939

DISCLAIMER

This book was prepared as an account of work sponsored by an agency of the United States Government. Neither the United States Government nor any agency thereof, nor any of their employees, makes any warranty, express or implied, or assumes any legal liability or responsibility for the accuracy, completeness, or usefulness of any information, apparatus, product, or process disclosed, or represents that its use would not infringe privately owned rights. Reference herein to any specific commercial product, process, or service by trade name, trademark, manufacturer, or otherwise, does not necessarily constitute or imply its endorsement, recommendation, or favoring by the United States Government or any agency thereof. The views and opinions of authors expressed herein do not necessarily state or reflect those of the United States Government or any agency thereof.

DISTRIBUTION OF THIS DOCUMENT IS UNLIMITED  
MOW

## **DISCLAIMER**

**This report was prepared as an account of work sponsored by an agency of the United States Government. Neither the United States Government nor any agency Thereof, nor any of their employees, makes any warranty, express or implied, or assumes any legal liability or responsibility for the accuracy, completeness, or usefulness of any information, apparatus, product, or process disclosed, or represents that its use would not infringe privately owned rights. Reference herein to any specific commercial product, process, or service by trade name, trademark, manufacturer, or otherwise does not necessarily constitute or imply its endorsement, recommendation, or favoring by the United States Government or any agency thereof. The views and opinions of authors expressed herein do not necessarily state or reflect those of the United States Government or any agency thereof.**

## **DISCLAIMER**

**Portions of this document may be illegible in electronic image products. Images are produced from the best available original document.**

NOTICE

This report was prepared as an account of work sponsored by the United States Government. Neither the United States nor the United States Department of Energy, nor any of their employees, nor any of their contractors, subcontractors, or their employees, makes any warranty, express or implied, or assumes any legal liability or responsibility for the accuracy, completeness, or usefulness of any information, apparatus, product or process disclosed or represents that its use would not infringe privately owned rights.

THIS PAGE  
WAS INTENTIONALLY  
LEFT BLANK

## ABSTRACT

A theoretical and experimental investigation of OH saturated fluorescence is described. The goal of the research is to develop a saturated fluorescence technique which will yield accurate molecular number densities over a wide range of flame pressure, temperature, and composition. The hydroxyl radical is an important species in all practical flames. Because its spectrum, radiative transfer rates and collisional transfer rates are unusually well-characterized, it serves as a model molecule for a detailed saturated fluorescence investigation. Experimentally, OH is excited by a ten nanosecond pulse from a Nd:YAG-pumped dye laser tuned to an isolated rotational transition in the (0,0) band of the  $A^2\Sigma^+ - X^2\Pi$  electronic system. The resulting fluorescence signal is resolved both spectrally and temporally. Total OH number densities are calculated by collecting fluorescence from the directly excited upper rotational level, and using the balanced cross-rate model to analyze the experimental data. The balanced cross-rate model is especially appropriate for the analysis of saturated fluorescence data when the pulse length of the excitation laser is on the order of nanoseconds, although its use is not restricted to such short pulse lengths. Fluorescence measurements of OH number density agree to within a factor of three with the results of independent OH absorption measurements. Significantly, the ratio of the fluorescence signal to the number density measured by absorption is nearly the same in 30, 100 and 250 torr  $H_2/O_2/N_2$  flat flames, demonstrating the insensitivity of

THIS PAGE  
WAS INTENTIONALLY  
LEFT BLANK

the saturated fluorescence signal to the quenching environment of the radical. Collisional transfer in excited OH is studied by recording the time development of OH fluorescence spectrum. The experimental spectra are compared with the results of time-dependent computer modeling. By varying rotational transfer rates until the calculated and experimental spectra agree, rotational transfer cross sections can be calculated. The signal processing system was thoroughly checked by comparing the photomultiplier output to that of a fast photodiode, and by comparing single pulse Rayleigh scattering and fluorescence traces with sampling oscilloscope traces.

PAH compounds are important because they are carcinogenic and may be precursors to soot formation in flames. The development of laser fluorescence techniques to measure PAH compound is complicated due to the complexity of PAH spectra and the wide variety of PAH compounds which can be formed during combustion. Narrowband laser excitation around 300 nm has been selected as most likely to allow species selectivity in PAH fluorescence detection.

Table of Contents

	Page
1. Introduction.....	1
2. Summary of Progress.....	3
3. Experimental Facility - The Flame Chemistry Laboratory.....	5
3.1 Subatmospheric Flat Flame Burner.....	5
3.2 Nd:YAG Laser System.....	7
4. Experimental and Theoretical Progress.....	8
4.1 Experimental System for Fluorescence Measurements.....	8
4.2 Saturated OH Fluorescence in Subatmospheric $H_2/O_2/N_2$ Flat Flames.....	11
4.3 Signal Processing System.....	23
4.4 Time-Resolved Rotational Transfer Studies.....	28
4.5 Fluorescence Measurements of Polycyclic Aromatic Hydrocarbons.....	31
5. Planned Experimentation for the Remainder of the Contract Year.	34
6. Effort of Research Personnel.....	34
7. Publication and Presentation of Work.....	35
7.1 Refereed Articles.....	35
7.2 Meeting Presentations.....	35
7.3 Other Presentations.....	36
8. References.....	37
9. Appendices	
9.1 Appendix 1. Balanced Cross-Rate Model.....	41
9.2 Appendix 2. Calculation of OH Number Densities from Saturated Fluorescence Data.....	48

## 1. Introduction

Radical species play a fundamental role in the chemical kinetics of flame processes. They account for the break up of the fuel and oxidizer and have a significant role in the formation of pollutants. Knowledge of their concentration and behavior is essential for detailed understanding of fundamental processes relevant to both energy conservation and pollutant control. Development of species specific, spatially resolved, sensitive molecular fluorescence techniques will provide experimental information required not only to demonstrate the validity of proposed combustion mechanisms but also to infer new mechanisms.

The primary goal of this research project is to develop a reliable molecular fluorescence technique which is applicable in a wide variety of flame conditions. Because of the insensitivity of the fluorescence signal to the quenching environment and laser power fluctuations, saturated fluorescence holds great promise as a rugged technique which will give reliable results over a wide range of flame temperature, pressure and composition. A key result of our research during the past year is that in three flames whose pressure varied by almost an order of magnitude, the ratio of the OH saturated fluorescence signal to the OH number density was nearly constant. In contrast to the saturated fluorescence signal, the OH fluorescence signal in the linear regime is inversely proportional to collisional transfer rates. To calculate collisional transfer rates and correct the linear

fluorescence signal to obtain accurate number densities, the flame pressure, temperature and composition would have to be measured. No such correction is necessary if the fluorescence signal is saturated.

To correctly interpret saturated fluorescence data for a given species, a detailed understanding of the laser excitation dynamics of the species is required. Once the excitation dynamics are understood, the fluorescence process can be modeled. Spectral and temporal regions of the fluorescence signal which can be reliably related to the desired total species number density can then be isolated. The balanced cross-rate model, which was developed during the 1979-1980 contract period, is used to analyze the saturated OH fluorescence data which is reported in this Progress Report. It appears to give reliable results over the range of flame conditions studied.

PAH compounds are important because they are potential carcinogens and may be precursors to soot formation in flames. Because new liquid fuels derived from coal or shale oil may have high aromatic content compared to petroleum-based fuels, formation of PAH compounds and soot will become even more of a problem in the future. The development of laser fluorescence techniques to measure PAH compounds is a challenging task due to the complexity of PAH spectra and the great number of PAH species which can be formed in a flame. A major goal of the research is to find spectral regions, both for excitation and fluorescence detection, which will allow the detection and measurement of

either individual PAH species or groups of PAH compounds with similar chemical structure.

## 2. Summary of Progress

The following was accomplished during the last contract year:

1. Saturated OH fluorescence was observed in subatmospheric  $H_2/O_2/N_2$  flames at pressures ranging from 30 to 250 torr. Number densities calculated from the saturated fluorescence measurements using the balanced cross-rate model (Lucht et al., 1980b) were within a factor of three of number densities calculated via OH absorption. In addition, the ratio of the OH number densities calculated by fluorescence and absorption was nearly the same in 30, 100 and 250 torr flames, demonstrating the insensitivity of the saturated fluorescence signal to the quenching environment of the OH radical.
2. The 1P20B photomultipliers and the signal processing system were thoroughly tested. The time response of the photomultipliers was checked by comparing their output with that of a fast photodiode; the temporal shape of the photodiode and photomultiplier signals was very similar. The validity of the signal averaging used to process the photomultiplier output was confirmed by using a 500 MHz real-time oscillo-

scope to capture the signal on a single pulse, and then averaging the digitized single pulse traces. The average of the single pulse traces closely approximated the sampling oscilloscope output.

3. The time development of the rotational distribution in  $A^2\Sigma^+(v=0)$  OH has been examined for a number of different flame pressures and excited transitions. The time-dependent spectra observed are compared with the spectra predicted by computer modeling of the laser excitation dynamics of OH using a rate equation approach outlined by Lucht and Laurendeau (1979). A rotational relaxation model proposed by Chan and Daily (1980) has been incorporated into the time-dependent computer code. By comparing the experimental and computer generated spectra, it should be possible to obtain collisional transfer cross sections for excited OH.
4. A literature review of PAH fluorescence was conducted, and the spectral region around 300 nm was selected as the one most likely to enable selective excitation of PAH species.
5. Horizontal and vertical motor drives for the flat flame burner were installed, and electronic read-outs of the burner position will be installed shortly. We will therefore be able to interface the burner positioning system with a microprocessor. The Nd:YAG-pumped dye laser system will be upgraded in March with the addition of a Nd:YAG amplifier and a dye laser post-amplifier.

### 3. Experimental Facility - The Flame Chemistry Laboratory

#### 3.1 Subatmospheric Flat Flame Burner

The flat flame burner was described in detail in the first two Progress Reports (Lucht et al., 1979; Lucht et al., 1980a). The flat flame burner system, shown in Figure 1, is ideal for the development of optical diagnostic techniques such as saturated fluorescence, because it provides well-characterized flames over a wide range of operating conditions. New techniques can therefore be thoroughly tested before they are applied to more complex combustion systems. Of course, the diagnostic techniques which are developed are of great value in fundamental chemical kinetics studies performed on the flat flame burner.

The flat flame burner consists of a sintered bronze disk 6 cm in diameter, on which premixed flames are stabilized, and a surrounding sintered bronze ring, through which diluent flows to prevent entrainment of ambient air. The burner is enclosed in an anodized aluminum pressure vessel designed for subatmospheric operation. The pressure vessel has four ports which are fitted with quartz flats for optical access. The pressure vessel is evacuated by a Kinney KDH-80 vacuum pump.

Flames have been stabilized on the burner over a wide range of pressure (15-760 torr), equivalence ratio (0.1-2.0) and diluent-to-oxidizer ratio (0.2-6.0). The day-to-day reproducibility of burner operating conditions has been verified by OH

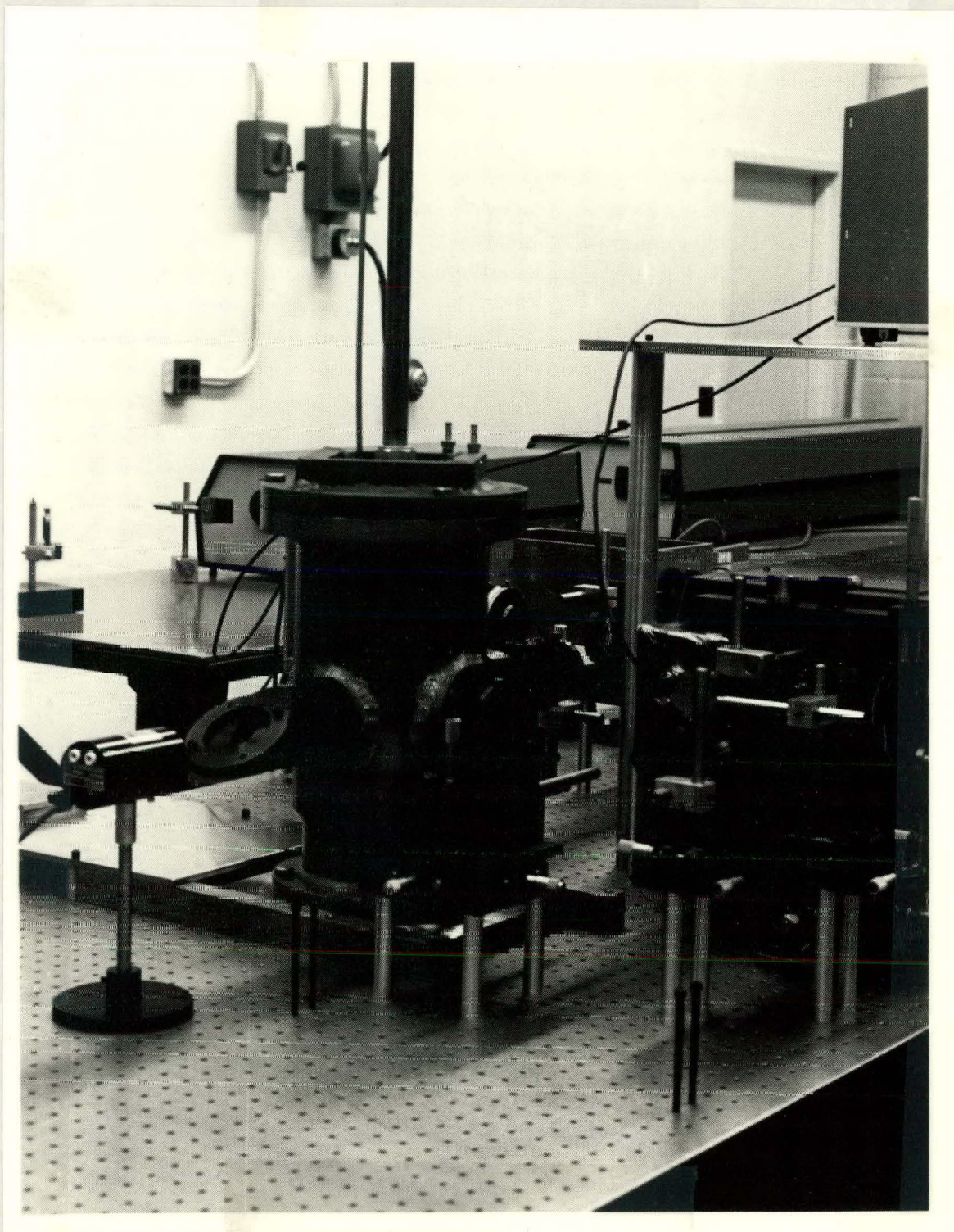


Figure 1. Experimental system. The flat flame burner is enclosed in the pressure vessel in the foreground. The Nd:YAG and dye lasers are visible in the background.

absorption measurements. The short term stability of the flame has been confirmed by monitoring the output of a miniature thermocouple with an oscilloscope.

During the past year, the flat flame burner system was mounted on a Newport Research optical table. Horizontal and vertical motor drives for the burner were installed. At present, the horizontal and vertical positions of the burner are read from dial indicators, but linear transducers will be installed shortly to give an electronic read-out of burner position. The addition of the motor drives and the linear transducers will allow the interfacing of the burner system with a microprocessor.

### 3.2 Nd:YAG Laser System

The Nd:YAG-pumped dye laser system has operated very well for the past year. During the first year of laser operation, the Nd:YAG laser kept drifting out of alignment after about an hour of operation. Molelectron added a stabilizing vertical plate to the Nd:YAG laser, and since then the alignment and power have been much more stable. Because the types of experiments performed using the laser require signal averaging, pulse to pulse temporal and energy stability of the laser are crucial. The temporal shape and energy of the laser pulse have been found to be stable over time periods as long as six hours.

The laser system will be upgraded in March with the addition of a Nd:YAG amplifier and a dye laser post-amplifier. The funds

for the amplifiers were provided by DOT Contract #DOT-RC-92004 in anticipation of PAH fluorescence measurements. The addition of the amplifiers will increase the laser power in the ultraviolet by approximately an order of magnitude. In addition, the beam quality of the dye laser output will be markedly improved because the last dye laser amplifier stage will be longitudinally pumped. Capital equipment funds are requested as part of the renewal proposal to purchase an etalon for the dye laser cavity to reduce the frequency bandwidth of the dye laser radiation from  $1 \text{ cm}^{-1}$  to  $.1 \text{ cm}^{-1}$ . The rationale for installing the etalon is further discussed in Section 4.3.

#### 4. Experimental and Theoretical Progress

##### 4.1 Experimental System for Fluorescence Measurements

The experimental system for OH fluorescence is shown schematically in Figure 2. Fluorescence is induced by tuning the dye laser radiation to an isolated transition in the (0,0) band of the  $A^2\Sigma^+ - X^2\Pi$  electronic system. The dye laser is pumped by the second harmonic (532 nm, 90 mJ) of the fundamental Nd:YAG laser beam (1064 nm, 250 mJ). The fundamental dye laser radiation (618 nm, 25 mJ) is doubled (309 nm, 2 mJ) using an angle tuned KDP crystal. The laser pulse length is nominally 10 nsec, but the pulse exhibits two or three lobes which have full widths at half maximum (FWHM) of 4 nsec.

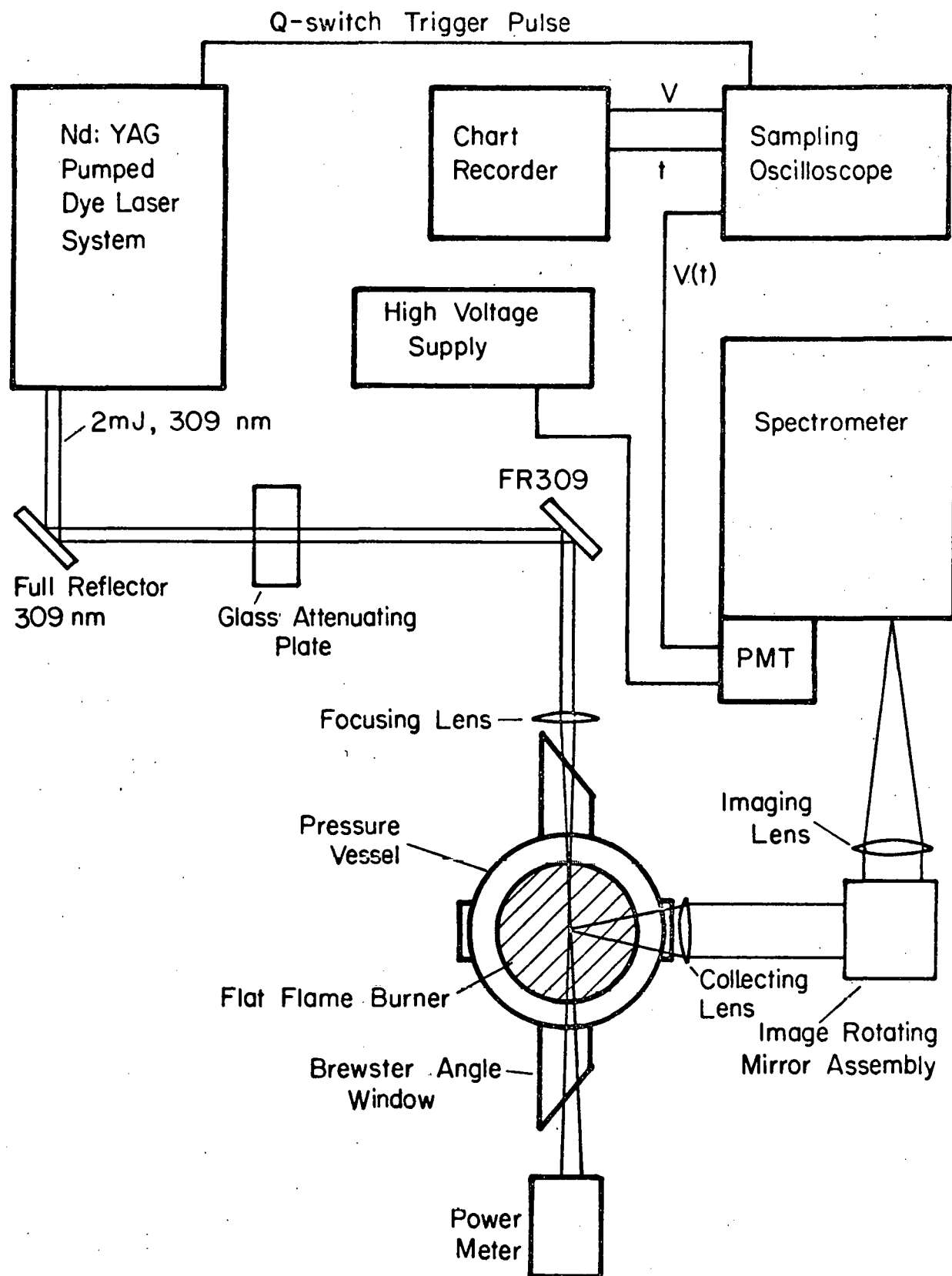


Figure 2. Experimental fluorescence system.

The dye laser radiation is reflected twice from dielectric mirrors which are full reflectors at 309 nm. The reflectance of the mirrors at 618 nm is approximately 10%, so that after two reflections the red energy in the beam is much less than a millijoule. The beam is then focused over the flat flame burner using a 30 cm quartz lens. The spot size at focus is on the order of 100  $\mu\text{m}$ , as measured by burn patterns on thermal paper.

OH fluorescence is collected by a 15 cm focal length quartz lens at right angles to the laser beam. The fluorescence image is rotated from a horizontal plane to a vertical plane using a two mirror system, and focused onto the vertical spectrometer slit by a 25 cm focal length quartz lens. The spectrometer slits are typically set at 75  $\mu\text{m}$ , and the resulting spectral resolution is approximately  $2 \text{ cm}^{-1}$ . A 1P28B photomultiplier specially wired so that the FWHM of the impulse response is 2 ns (Harris et al., 1976) is placed at the exit slit. The photomultiplier signal is processed by a 1 GHz Tektronix 5S14N sampling oscilloscope. The 5S14N sampling window can be scanned across or placed at a given time position in the fluorescence pulse waveform. The time position and vertical deflection of the sampling window are displayed on a chart recorder. A capacitor is placed across the chart recorder leads to minimize random noise in the recorded signal.

#### 4.2 Saturated OH Fluorescence in Subatmospheric H<sub>2</sub>/O<sub>2</sub>/N<sub>2</sub> Flat Flames

In the Progress Report (Lucht et al., 1980a) for the contract period 3-1-79 to 2-29-80, the so-called balanced cross-rate model was outlined. The balanced cross-rate model was proposed in order to analyze saturated fluorescence data when the exciting laser pulse length is on the order of nanoseconds. During the past year, the balanced cross-rate model was used to calculate OH number densities from saturated fluorescence measurements in subatmospheric H<sub>2</sub>/O<sub>2</sub>/N<sub>2</sub> flat flames. The OH number densities calculated from the fluorescence measurements showed good agreement with number densities calculated via absorption measurements in three flames whose pressure varied by nearly an order of magnitude, 30, 100 and 250 torr flames.

Briefly reviewing the balanced cross-rate model, the basic premise is that fluorescence from the single upper rotational level which is directly excited by the laser can be reliably related to the total molecular population, provided that the total population of the single upper and lower rotational levels coupled by the laser transition is constant during the laser pulse. Because the laser-induced transitions that couple the directly excited levels are so fast at saturation conditions, a steady state population balance is established between these two levels in less than a nanosecond. Therefore, the populations of the directly excited upper and lower levels can be related using a simple two level saturation model. The total population of the

directly excited upper and lower levels will be nearly constant during the laser pulse because the population depletion of the system via rotational relaxation out of the upper level will be approximately balanced by the population gain due to rotational relaxation into the lower level. The total population of the two level system is found by analyzing the fluorescence signal from the directly excited upper level; this total population is equal to the population of the directly excited lower level prior to excitation. The total molecular population can then be calculated from the population of the directly excited lower rotational level using Boltzmann statistics. The balanced cross-rate model can be applied even when the laser pulse is long relative to characteristic collisional transfer times, but is especially appropriate when the laser pulse is short and rotational steady state is not approached. The balanced cross-rate model is described in more detail in a paper published in Applied Optics (Lucht et al., 1980b), a reprint of which is included as Appendix 1.

An OH excitation and fluorescence detection scheme appropriate for the balanced cross-rate model is illustrated in Figure 3. The laser is tuned to the  $P_1(5)$  rotational transition in the  $(0,0)$  band of the  $A^2\Sigma^+ - X^2\Pi$  electronic system. Fluorescence from the directly excited upper level is detected by tuning the spectrometer to the  $Q_1(4)$  line. By observing fluorescence at a different wavelength than the exciting laser radiation, interference due to Rayleigh scattering is avoided. A typical laser pulse and

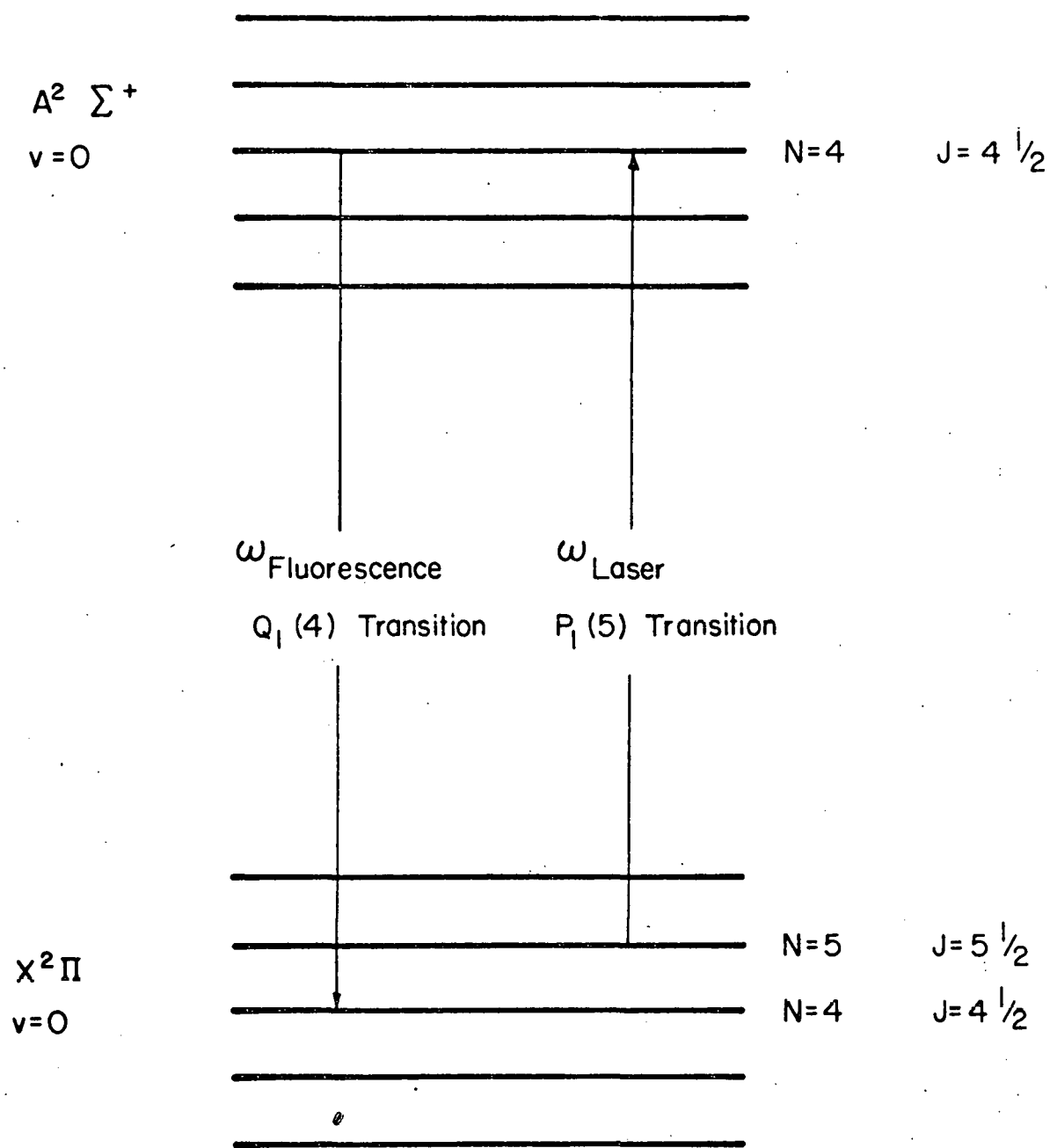


Figure 3. OH excitation and fluorescence detection scheme.

the corresponding laser-induced fluorescence pulse are shown in Figure 4. The laser pulse was recorded by filling the pressure vessel with 20 torr of room temperature  $N_2$  and tuning the spectrometer to the laser wavelength to observe Rayleigh scattering from the nitrogen.

The saturated fluorescence measurements are performed by placing the sampling window at the peak of the first lobe of the fluorescence pulse. The sampler puts out a voltage proportional to the vertical deflection of the window. An average voltage is obtained by integrating for approximately two minutes. By attenuating the laser beam using calibrated Pyrex plates of various thicknesses, a fluorescence versus transmission curve is generated. Typical curves are shown for 30 and 250 torr  $H_2/O_2/N_2$  flames in Figure 5. At both pressures, substantial saturation of the fluorescence signal occurs. The water vapor pressure in the 250 torr  $H_2/O_2/N_2$  flame is 143 torr, the same as in an atmospheric pressure, stoichiometric methane-air flame. Because water vapor has the highest cross section for OH electronic quenching,  $50 \text{ \AA}^2$  versus  $15 \text{ \AA}^2$  for  $CO_2$  and  $5 \text{ \AA}^2$  for  $N_2$  (Chan and Daily, 1980), the saturation behavior of OH in the 250 torr  $H_2/O_2/N_2$  flame is similar to the saturation behavior in a one atmosphere methane-air flame.

The data is extrapolated to the condition of full saturation by plotting fluorescence versus inverse transmission (transmission is directly proportional to laser power) and fitting a line through the points, as shown in Figure 6. The y-intercept is the

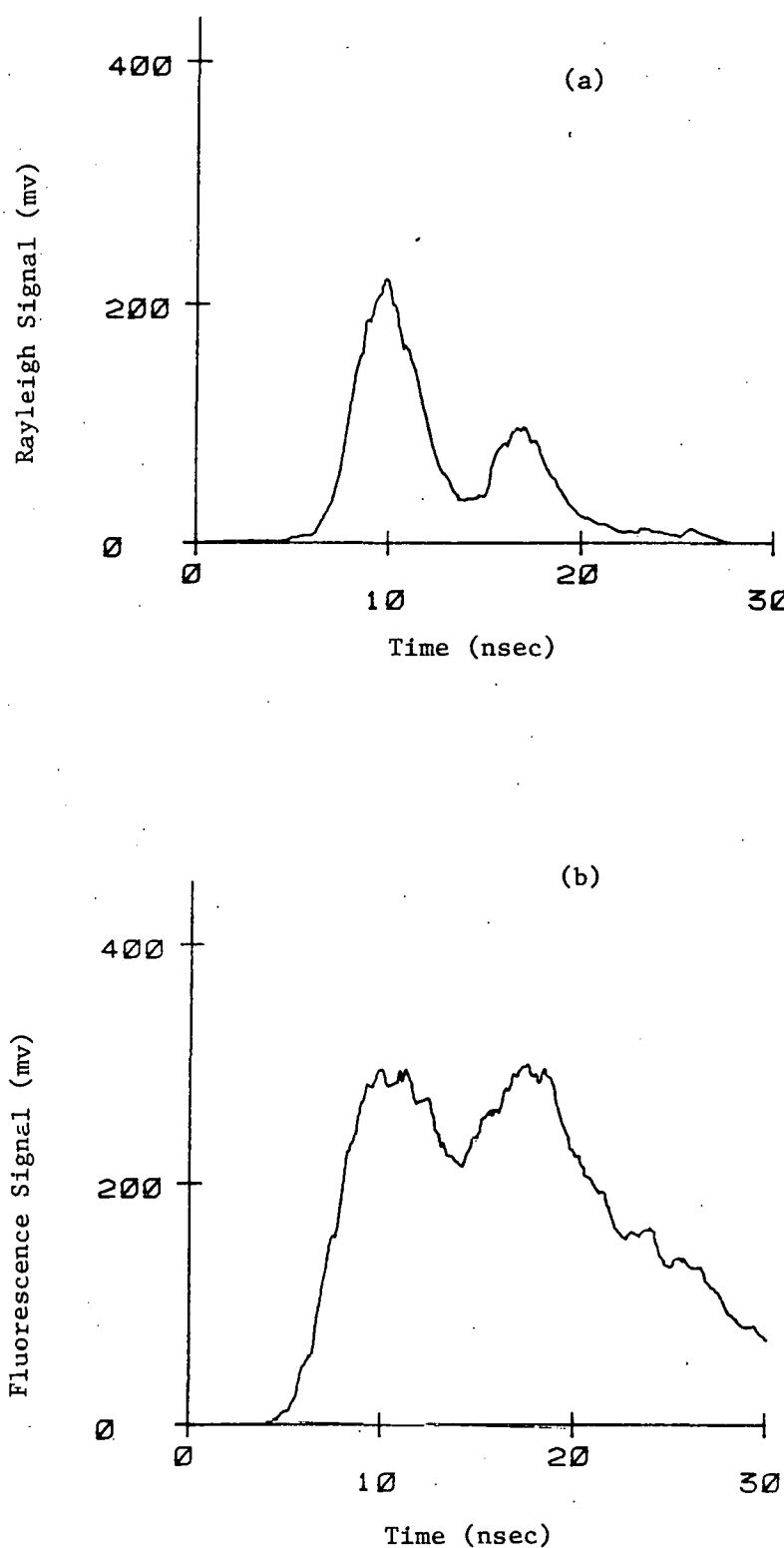


Figure 4. Sampling oscilloscope traces of (a) Rayleigh scattering from the laser pulse and (b) laser induced fluorescence from the  $Q_1(4)$  transition. The laser was tuned to the  $P_1(5)$  transition. The  $H_2/O_2/N_2$  flame pressure was 30 torr.

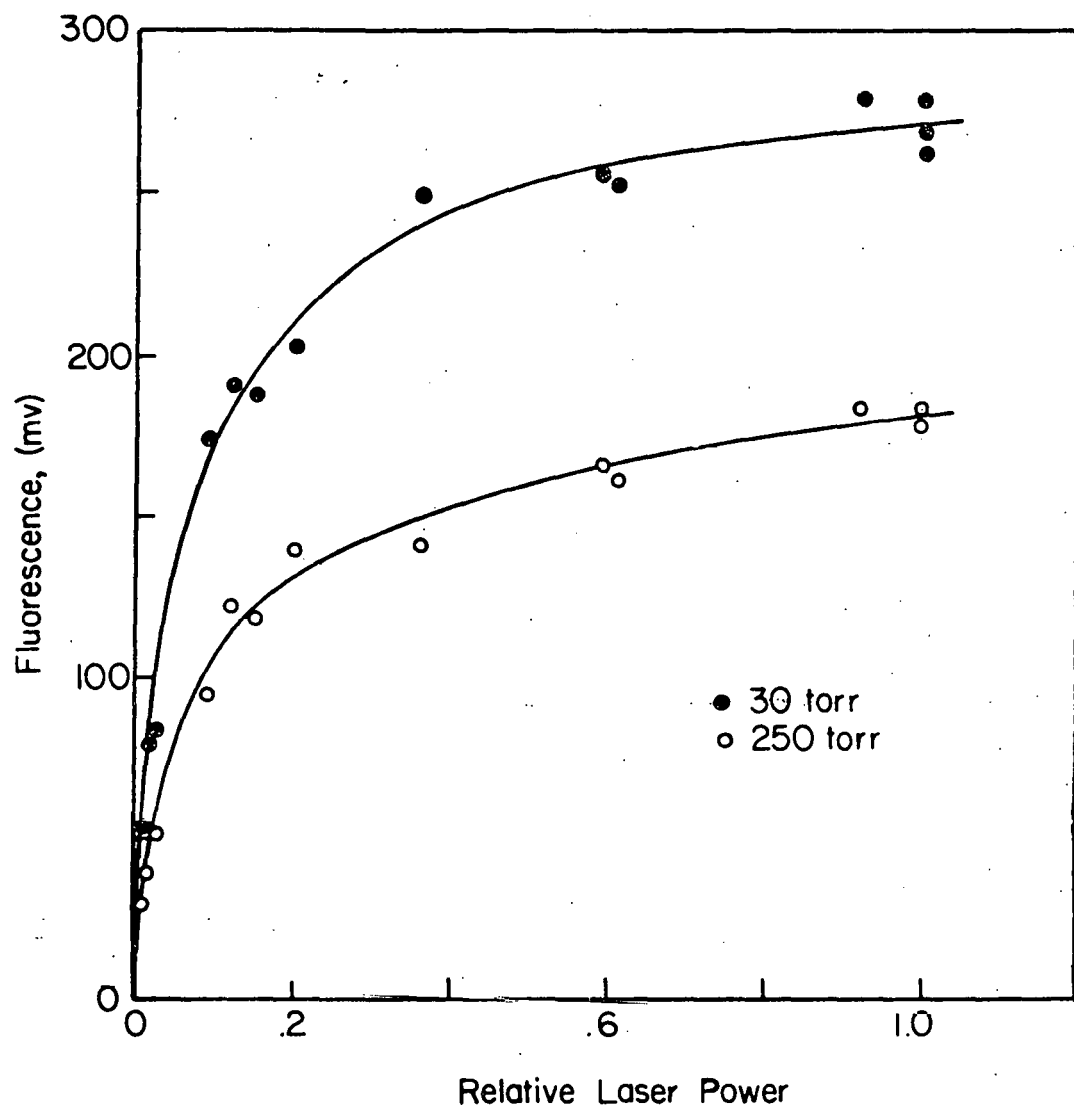


Figure 5. OH fluorescence versus relative laser power in 30 and 250 torr  $H_2/O_2/N_2$  flames.  $P_1(5)$  excitation,  $Q_1(4)$  fluorescence.

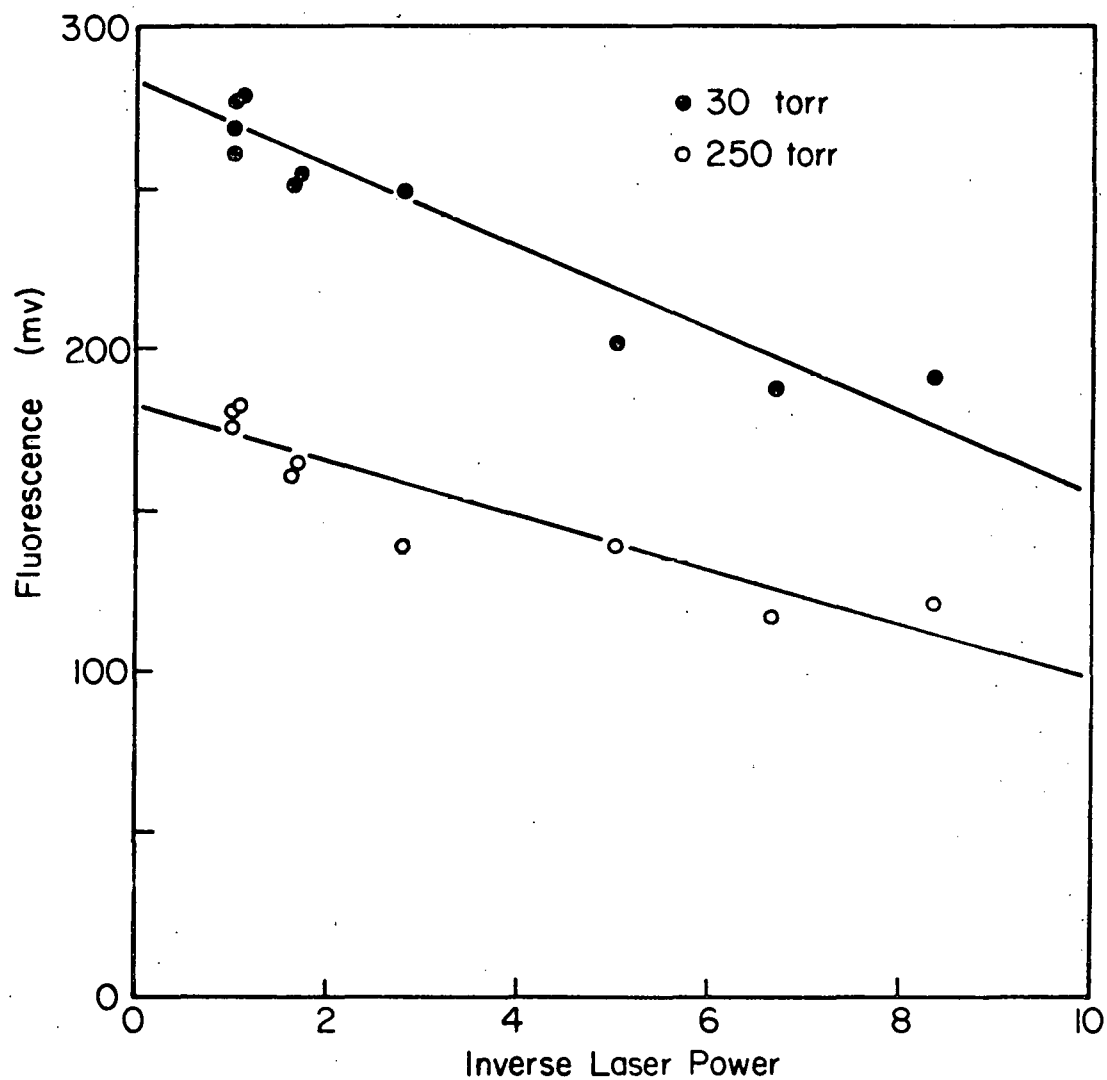


Figure 6. OH fluorescence versus inverse laser power for 30 and 250 torr  $\text{H}_2/\text{O}_2/\text{N}_2$  flames.  $\text{P}_1(5)$  excitation,  $\text{Q}_1(4)$  fluorescence.

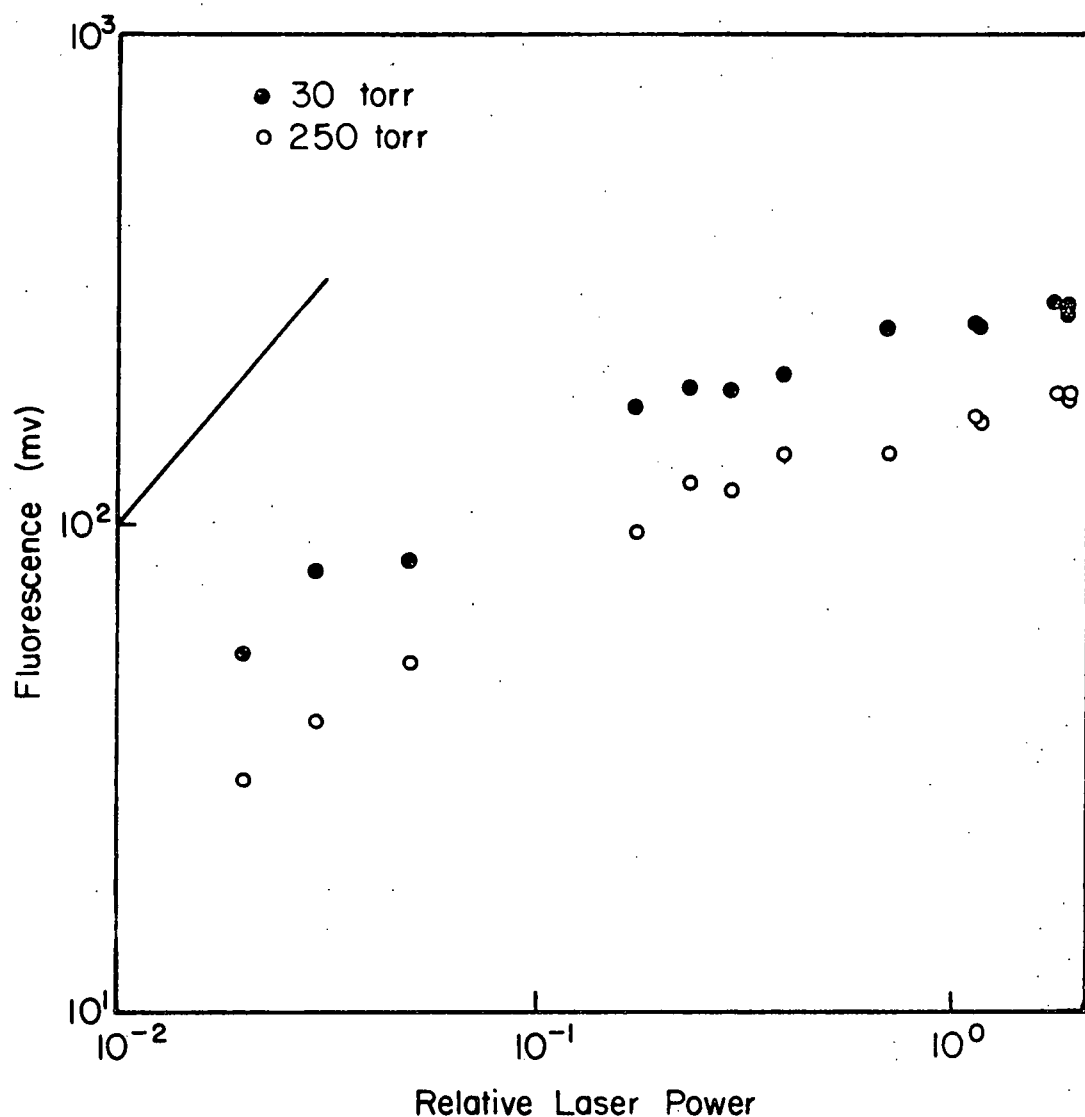


Figure 7. OH fluorescence versus relative laser power, log-log plot, in 30 and 250 torr H<sub>2</sub>/O<sub>2</sub>/N<sub>2</sub> flames. P<sub>1</sub>(5) excitation, Q<sub>1</sub>(4) fluorescence. The slope of the solid line is the slope which linear fluorescence data would have.

fluorescence signal at  $(\text{transmission})^{-1}=0$ , or infinite laser power. This method of extrapolating the near saturated fluorescence data to the condition of full saturation was suggested by Baronavski and McDonald (1977), who did not at that time consider the effect of the laser beam intensity profile on the shape of the saturation curve (Daily, 1978; Pasternack et al., 1979; Lucht, 1979). However, determining the actual intensity profile at laser focus and correctly accounting for the geometry of the fluorescence collection optics, which will also affect the slope of the saturation curve, are extremely difficult tasks. The intercept of the saturation curve is not, however, affected by these factors (Lucht, 1979). The simple Baronavski and McDonald extrapolation is used; the test of the extrapolation is the comparison of number densities calculated via fluorescence and absorption methods. The calculation of number densities from the saturated fluorescence data is outlined in Appendix 2. Table 4.1 lists OH number densities calculated independently from absorption and fluorescence. The number densities calculated from fluorescence are a factor of three higher than those calculated from absorption; the probable reason for this difference is the difficulty of correctly estimating the cross-sectional area of the fluorescence collection volume.

The absorption measurements are accurate to  $\pm 10\%$  (Lucht, 1979), but because absorption is a path averaged measurement the OH number density at the center of the burner will be higher than the number density calculated from the absorption measurement.

Horizontal scans of the burner using fluorescence have been made, and the OH number density does fall gradually as the edge of the burner is approached. To analyze the burner scans correctly, however, self-absorption of the fluorescence signal, which is approximately 10% when the center of the burner is probed, must be taken into account. At this time the analysis is incomplete, but based on the gradually changing OH number density profile observed, it is unlikely to account for the discrepancy in the fluorescence and absorption results. In a study of CN and CH saturated fluorescence, Eckbreth et al. (1979) also found that the number densities which they calculated from their saturated fluorescence measurements were a factor of two higher than those calculated via absorption.

It is very significant, however, that the ratios of the number densities calculated from fluorescence and absorption are nearly equal for all three flames, despite a factor of eight change in flame pressure and collisional transfer rates. The constant number density ratio strongly suggests that the discrepancy between the absorption and fluorescence results is due solely to the difficulty in accurately estimating the fluorescence collection volume, and not to errors in modeling OH laser excitation dynamics. This is good evidence for the validity of the balanced cross-rate model and the usefulness of the Baronavski and McDonald extrapolation. It also demonstrates the insensitivity of the saturated fluorescence technique to the quenching environment of the OH radical. The fluorescence-to-

21

absorption ratio given in Table 4.1 can be regarded as a calibration factor which takes into account the geometry of the fluorescence collection system. Once this calibration factor is measured for one flame condition, it can be used to calculate OH number densities from saturated fluorescence data over a wide range of flame conditions.

Flame Pressure	Water Vapor Pressure	Fluorescence	Absorption	OH Number Density
		( $10^{15} \text{ cm}^{-3}$ )	( $10^{15} \text{ cm}^{-3}$ )	Fluor/Abs
30	17	4.7	2.0	2.4
100	57	4.6	1.5	3.0
250	143	3.1	1.2	2.6

Table 4.1 OH number densities calculated from independent saturated fluorescence and absorption measurements.

The normalized slopes of the near saturated Baronavski and McDonald plots (Figure 6) for the six flame conditions studied are given in Table 4.2. The normalized slope is simply the slope of the line fitted to the fluorescence versus inverse transmission data divided by the y-intercept of the line. The greater the magnitude of the normalized slope, the harder it is to saturate the  $P_1(5)$  transition. Note that the normalized slope is not an increasing function of pressure, as one might expect from a simple two level rate equation analysis of saturation (Daily, 1977; Baronavski and McDonald, 1977). Instead, the slope is a minimum at 80 torr. To fully explain this intriguing result, the

axial mode structure of the dye laser and homogeneous and inhomogeneous broadening of the OH resonance must be considered. It is interesting to note from Table 4.2 that the minimum in normalized slope is reached when the FWHM of the homogeneous OH linewidth is approximately one-half the laser axial mode spacing. Below this pressure, a significant fraction of the OH molecules would be in Doppler intervals which would not interact strongly with the laser radiation. The transition would thus be much more difficult to saturate (Piepmeier, 1972a, 1972b; Killinger et al., 1976). We are presently undertaking a theoretical study of the interaction of multi-mode laser radiation and an OH resonance using density matrix methods. The goal of the study is to quantitatively predict the saturation behavior of the resonance.

Flame Pressure (Torr)	Homogeneous FWHM (cm <sup>-1</sup> )	Normalized slope
30	.005	-.0454
50	.008	-.0432
80	.013	-.0404
100	.016	-.0446
150	.024	-.0442
250	.040	-.0470

Table 4.2. Normalized slope of the Baronavski and McDonald plot as a function of flame pressure and OH homogeneous linewidth (Wang et al., 1980). The normalized slope is the slope divided by the y-intercept. The mode spacing of the dye laser is  $\approx .03\text{cm}^{-1}$ .

#### 4.3 Signal Processing System

The temporal response of the 1P28B photomultiplier used to detect fluorescence and Rayleigh scattering pulses was checked by comparing their output with that of a fast photodiode (Scientech Model 301-020) which has a claimed resolution of less than a nanosecond. Single pulse traces of the photodiode output and the 1P28B output due to Rayleigh scattering are shown in Figure 8. The pulses were recorded with a 500 MHz storage oscilloscope (Tektronix 7834). The temporal shape of the pulses are very similar, and the FWHM of the lobes in the laser pulse are approximately 4 nsec, as claimed by Molelectron.

The signal processing system was also checked by averaging approximately ten consecutive single pulse traces by digitizing the traces and performing the averaging numerically. The average of the single pulse traces was then compared to the sampling oscilloscope traces for fluorescence, Rayleigh scattering, and the photodiode output. Single pulse, averaged single pulse, and sampling oscilloscope traces are shown for fluorescence in Figure 9 and for Rayleigh scattering in Figure 10. In both cases the average of the single pulse traces closely approximates the sampling oscilloscope traces, confirming the validity of the signal averaging procedure described in Section 4.1.

The single pulse fluorescence traces consistently showed more pulse-to-pulse variation and exhibited more noise during the pulse than did the Rayleigh scattering pulses, even though the

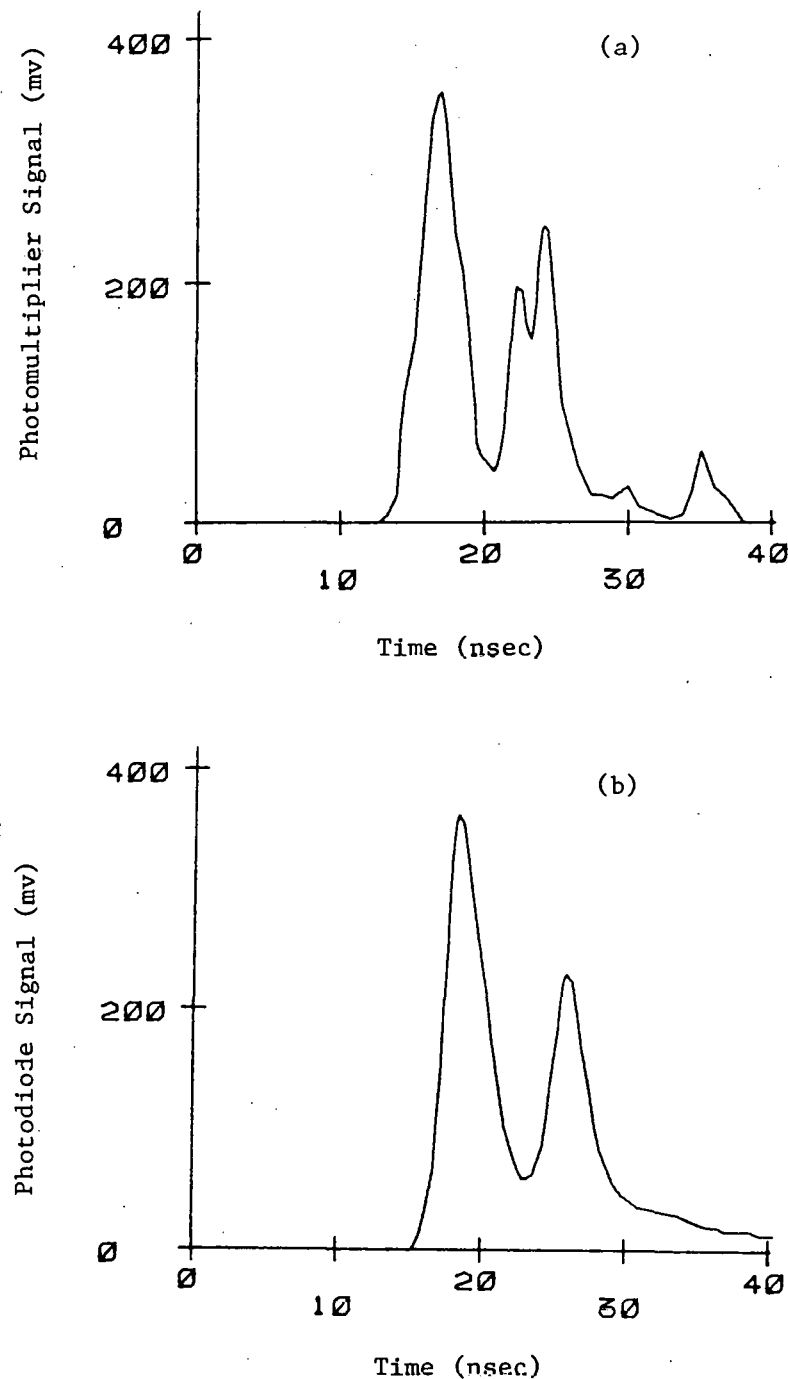


Figure 8. (a) Single pulse photomultiplier output due to Rayleigh scattering and (b) Single pulse photodiode output. The laser frequency was  $32236 \text{ cm}^{-1}$ .

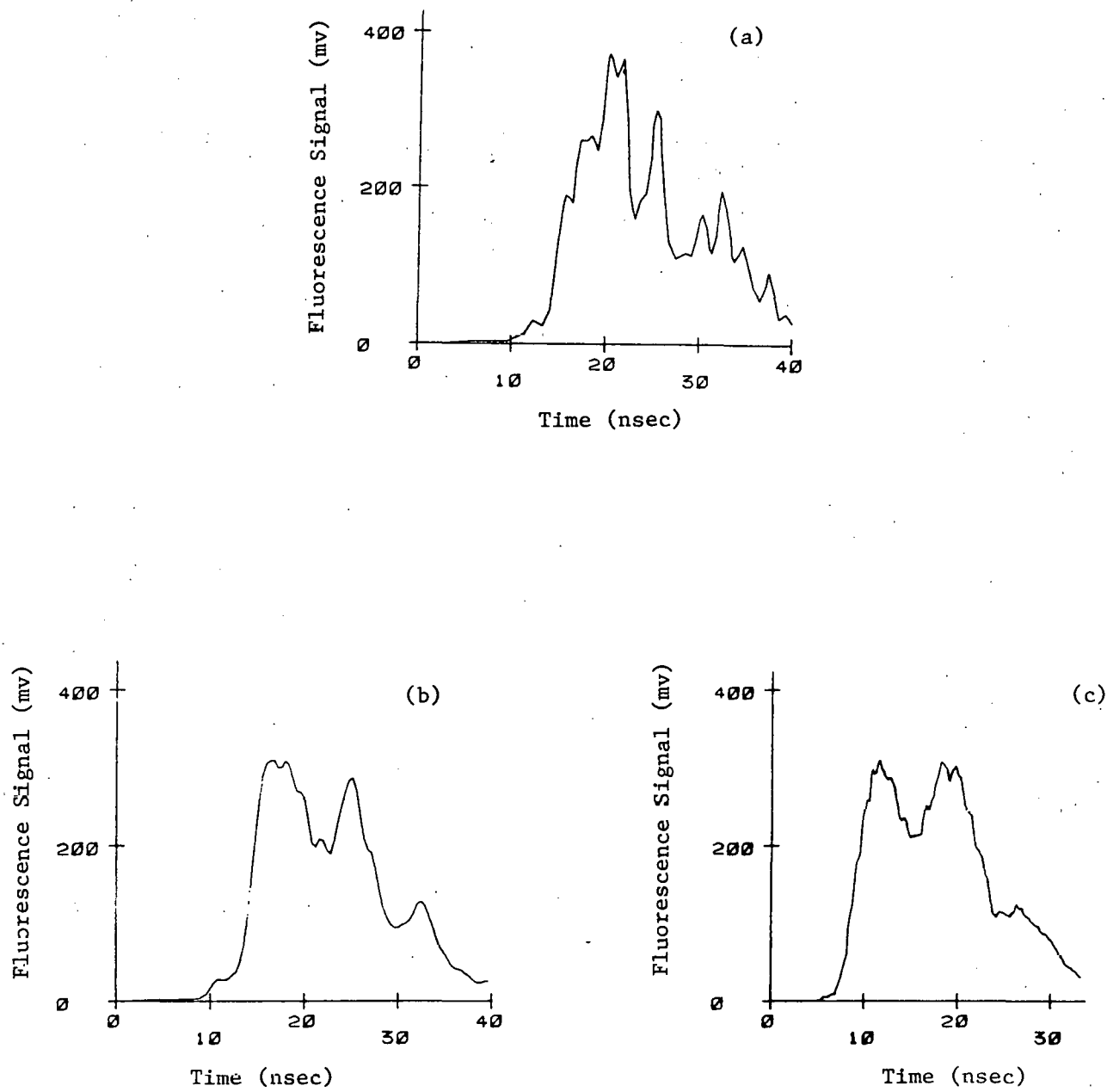


Figure 9. (a) Single pulse, (b) averaged single pulse, and (c) sampling oscilloscope traces of the  $Q_1(4)$  fluorescence signal. The  $P_1(5)$  transition was excited. The  $H_2/O_2/N_2$  flame pressure was 50 torr.

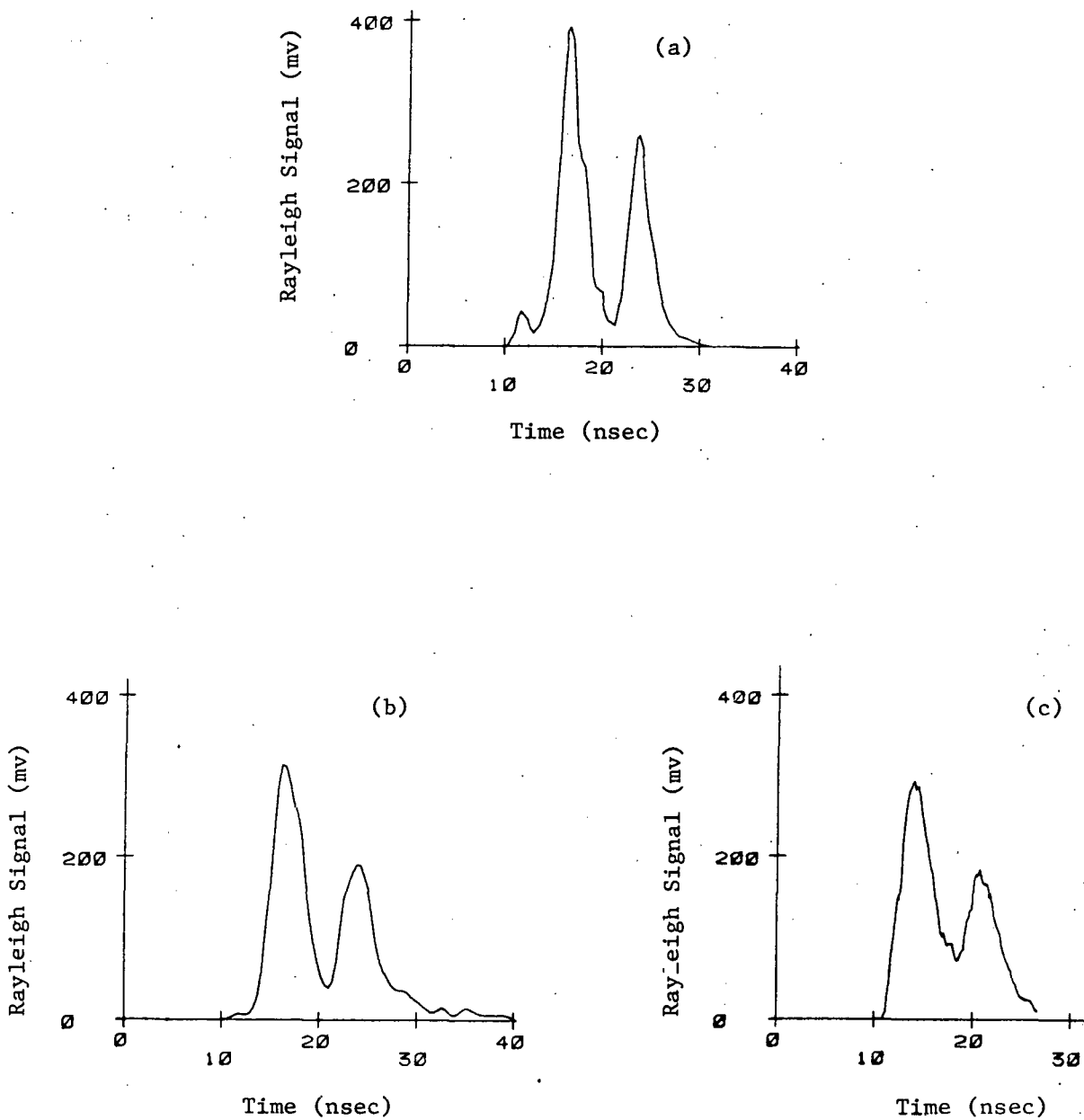


Figure 10. (a) Single pulse, (b) averaged single pulse, and (c) sampling oscilloscope traces of the Rayleigh scattering signal from 20 torr of room temperature  $N_2$ . The laser frequency was  $32236 \text{ cm}^{-1}$ .

- 7

same photomultiplier was used for both measurements and the signal level was nearly the same for both. The noise in the fluorescence pulse is possibly due to variations in the axial mode structure of the dye laser radiation. The dye laser, which has a frequency bandwidth of  $\approx 1\text{cm}^{-1}$ , has approximately twenty or thirty axial modes with a spacing of  $\approx 0.03\text{cm}^{-1}$ . Only some of these modes interact strongly with the OH absorption line, which has a FWHM due to Doppler broadening of  $0.25\text{ cm}^{-1}$ . Consequently, if there are variations in the intensity of the axial modes which excite the OH resonance, either during the laser pulse or pulse-to-pulse, the fluorescence signal would exhibit substantial random noise. This same noise would not appear in the Rayleigh scattering signal because the Rayleigh signal is proportional only to the total intensity of the laser axial modes, and is insensitive to the intensity distribution among those modes.

Funds for a pressure-tuned etalon for the dye laser cavity are requested in the renewal proposal. The etalon will reduce the dye laser bandwidth from  $\approx 1\text{cm}^{-1}$  to  $\approx 0.1\text{cm}^{-1}$ . As a result, the number of axial modes will be reduced such that all modes will interact strongly with the OH resonance. It is hoped that this will eliminate most of the high-frequency noise which is evident in the single pulse fluorescence traces of Figure 9, and make possible a demonstration experiment in which single pulse fluorescence traces are used to calculate OH number densities. Single pulse measurements are of great interest in turbulent combustion studies because probability density functions of flame

properties can be calculated from the single pulse data.

#### 4.4 Time-Resolved Rotational Transfer Studies

Rotational transfer in excited OH is studied by placing the sampling window at a given time position in the laser pulse waveform and scanning the spectrometer across the OH fluorescence band. A typical spectrum, recorded at the peak of the first lobe of a laser pulse, is shown in Figure 11. The time development of the rotational distribution is investigated by recording spectra at a number of different time positions in the laser pulse.

The experimental results are compared with the results of a time-dependent computer program which integrates the population transfer rate equations outlined in Lucht and Laurendeau (1979). Fifty-five OH rotational levels are considered, with rotational quantum number  $N \leq 14$  for the upper rotational levels and  $N'' \leq 13$  for the lower rotational levels. A rotational relaxation model proposed by Chan and Daily (1980) was recently incorporated into the computer program. The program calculates the time-dependent OH population distribution for a given laser temporal pulse shape. A subroutine then generates synthetic OH fluorescence spectra from the calculated population distribution among the upper rotational levels. Such a spectrum is shown in Figure 12.

The spectrum shown in Figure 12 was calculated at the peak of the first lobe of a laser pulse similar to the experimental laser pulse which produced the spectrum shown in Figure 11. The

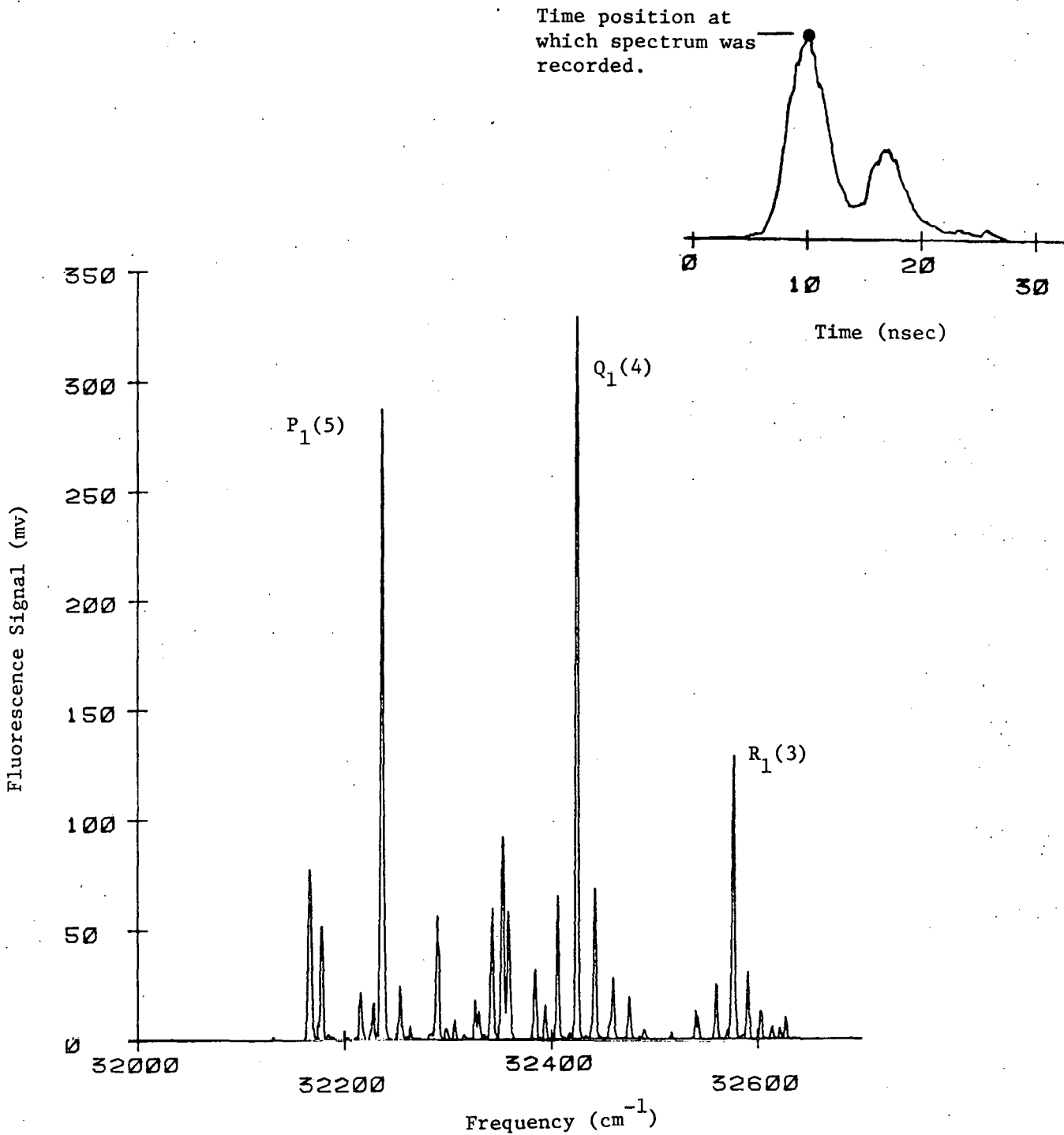


Figure 11. Experimental OH spectrum. The  $P_1(5)$  line was directly excited. The exciting laser pulse and the time position at which the spectrum was recorded are shown in the upper inset. The  $\text{H}_2/\text{O}_2/\text{N}_2$  flame pressure was 30 torr.

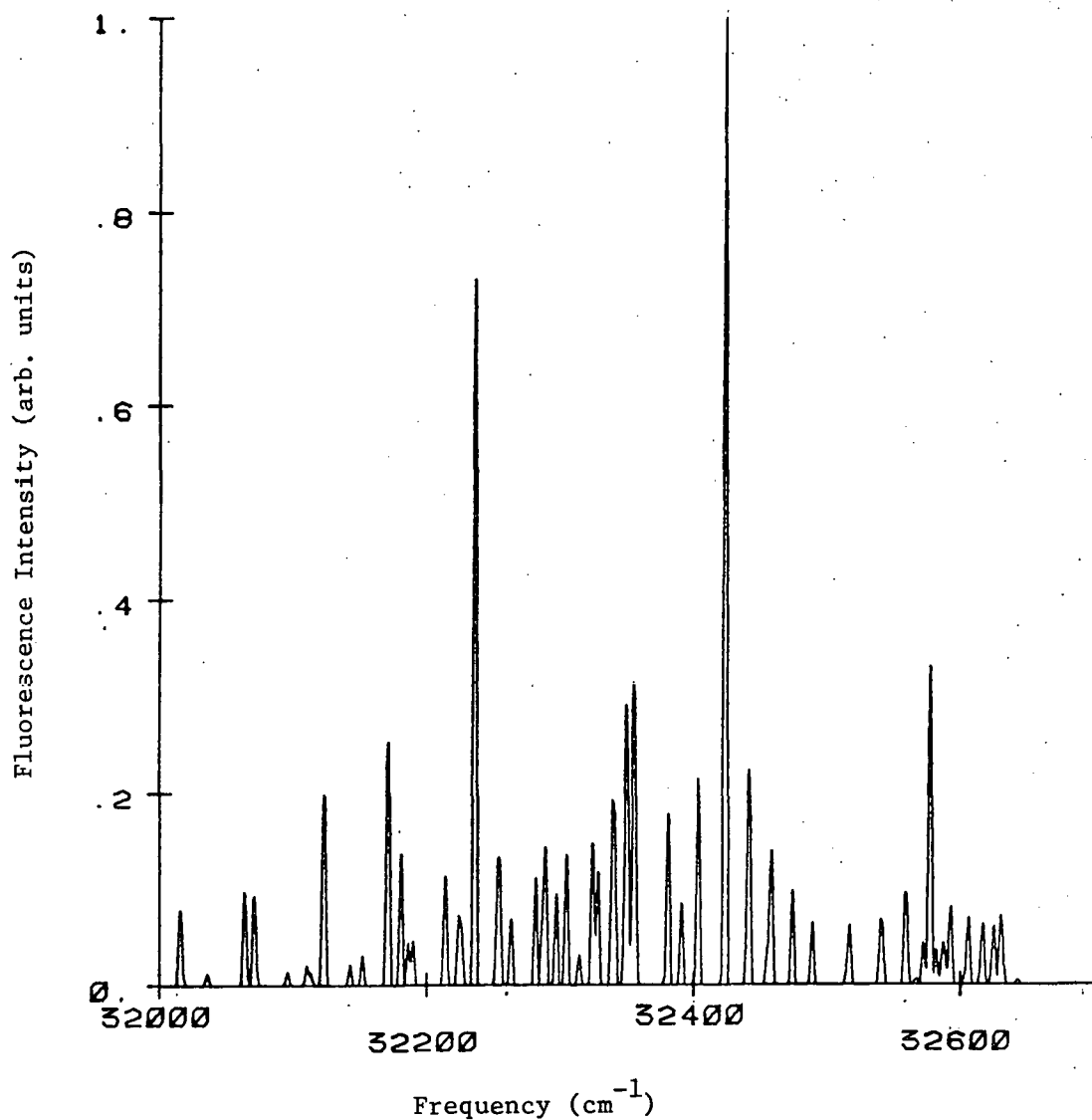


Figure 12. Calculated OH fluorescence spectrum. The spectrum shown was calculated at the same position in the laser pulse as the experimental spectrum shown in Figure 11.

experimental and calculated spectra are very similar qualitatively. At this time we have not attempted to optimize the agreement between experimental and calculated spectra by varying the rotational transfer cross-sections which are used to calculate rotational relaxation rates. By doing so, however, rotational relaxation cross-sections from given excited rotational levels can be calculated. Such computer studies will be pursued during the remainder of the contract period.

#### 4.5 Fluorescence Measurements of Polycyclic Aromatic Hydrocarbons

The goal of this research is to develop laser fluorescence techniques to measure PAH concentrations in flames. In initial calibration experiments, various PAH species will be vaporized directly into a heated diluent, which will then flow through the flat flame burner. Quartz probe sampling followed by capillary gas chromatography/mass spectroscopy can be used to validate the fluorescence technique. In later experiments, PAH compounds will be formed by adding small amounts of benzene to hydrogen-oxygen-argon flames stabilized on the flat flame burner.

Due to difficulties in finding a qualified graduate student, we are only beginning to develop procedures for PAH fluorescence measurements. Mr. Paul Ludington, a senior at Purdue, is now undertaking this task; he will begin graduate studies toward the Master's degree in June, 1981. A recent EPA grant focuses on the kinetics of aromatic combustion and PAH formation. The DOE work

will concentrate on development of a suitable *in situ* laser fluorescence technique using either the linear or the saturation regime.

A literature review has produced the following results and conclusions:

1. Fluorescence of PAH compounds occurs at 350-700 nm upon excitation at 250-500 nm (Richardson and Ando, 1977; Berlin, 1971). Narrowband laser excitation near 300 nm offers the best opportunity for species selectivity (Richardson and Ando, 1977). The fluorescence spectra of PAHs with substantial aliphatic substitution do not differ substantially from that of the unsubstituted parent compound; the fluorescence spectra of larger PAHs shift noticeably towards longer wavelengths. Separation of closely related PAHs is thus problematic; however, we can monitor PAHs of different ring size to see if PAH growth is related to soot formation. Spectral deconvolution is possible via known mass spectrometer methods.
2. Naphthalene, anthracene, phenanthrene, fluoranthene and pyrene are the primary PAH compounds observed in combustion processes. Typical gas-phase concentrations are 10 ppb - 10 ppm (France, 1979; Coe and Steinfield, 1980). Coe and Steinfield (1980) find that laser fluorescence in a flame is possible to at least 100 ppb; detectivity in a water environment is possible down to 100 ppt (Richardson and Ando,

1977).

3. Evidence is building for a connection between PAH and soot formation. Haynes et al. (1980) have recently found that the fluorescence signal from a premixed flat flame (assumed due to PAHs) drops to zero at a flame position coincident with the onset of soot formation. This result suggests that PAHs are important as both carcinogens and soot precursors.
4. Few vapor phase PAH fluorescence spectra are available in the literature. Initial measurements by Coe and Steinfield (1980) show that the laser induced fluorescence spectra of fluoranthene and pyrene are broad-band with little fine structure. Little change in spectral response occurs between room temperature and flame temperature conditions.

The addition of the Nd:YAG amplifier and dye laser post-amplifier will significantly increase the laser power at wavelengths of 350 nm and below, which appears to be the most promising excitation region for separation of various PAH species. The flow system to inject the PAH into heated diluent was developed as part of a pyridine kinetics study, and has been thoroughly calibrated and tested.

### 5. Planned Experimentation for the Remainder of the Contract

#### Year

Much of the remainder of the contract year will be devoted to analyzing the OH fluorescence data which has been collected in recent months. In particular, the fluorescence spectra observed experimentally will be compared to computer-generated spectra to calculate rotational relaxation cross sections.

NH saturated fluorescence will be investigated in methane/nitrous oxide/nitrogen or hydrogen/nitrous oxide/nitrogen flames, which should produce enough NH to be measurable by optical absorption. PAH fluorescence will be investigated in cold flow through the flat flame burner. A likely first candidate for such studies is naphthalene dissolved in hexane.

### 6. Effort of Research Personnel

Professors D.W. Sweeney and N.M. Laurendeau have devoted about 15% of their time to the contract during the academic year. Professor Laurendeau was on sabbatical last summer but Professor Sweeney contributed about 25% of his time to the research effort. Mr. R.P. Lucht was a full-time PhD graduate research assistant on the project for the full contract year.

## 7. Publication and Presentation of Work

During the past year, our work has been published or presented as follows:

### 7.1 Refereed Articles

- [1] R.P. Lucht, D.W. Sweeney and N.M. Laurendeau, "Saturated Fluorescence Measurement of the Hydroxyl Radical," in Laser Probes for Combustion Chemistry, D.R. Crosley, Ed., ACS Symposium Series 134, Washington, D.C., 1980.
- [2] R.P. Lucht, D.W. Sweeney and N.M. Laurendeau, "Balanced Cross-Rate Model for Saturated Molecular Fluorescence in Flames Using a Nanosecond Pulse Length Laser," Applied Optics 19, 3295, 1980.

### In preparation:

- [3] R.P. Lucht, D.W. Sweeney and N.M. Laurendeau, "Saturated Fluorescence Measurement of OH in Subatmospheric Flat Flames," to be submitted to Combustion and Flame.

### 7.2 Meeting Presentations

- [1] R.P. Lucht, D.W. Sweeney and N.M. Laurendeau, "Saturated Fluorescence Measurement of OH in Subatmospheric Flat Flames," Molecular Spectroscopy Symposium, Columbus, Ohio, June, 1980.

1/16 5/1

In preparation:

[ 3] R.P. Lucht, D.W. Sweeney and N.M. Laurendeau, "Time-Resolved, Saturated Fluorescence Measurement of OH," Gordon Conference on Chemistry and Physics of Laser Diagnostics in Combustion, Plymouth, New Hampshire, June, 1981.

7.3 Other Presentations

Professor Sweeney presented a seminar on our work at the University of Michigan in March, 1981.

### 8. References

A.P. Baronavski and J.R. McDonald (1977), Appl. Opt. 16,  
1897.

I.B. Berlman (1970), Handbook of Fluorescence Spectra  
of Aromatic Molecules, Academic Press, New York.

P.A. Bonczyk and J.A. Shirley (1979), Comb. and Flame 34,  
253.

C.K. Chan and J.W. Daily (1980), Appl. Opt. 19, 1357.

D.S. Coe and J.I. Steinfeld (1980), in Laser Probes for  
Combustion Chemistry, ACS Symposium Series 134, D.R. Crosley,  
Ed., American Chemical Society, Washington, D.C.

J.W. Daily (1977), Appl. Opt. 16, 568.

J.W. Daily (1978), Appl. Opt. 17, 225.

A.C. Eckbreth, P.A. Bonczyk and J.F. Verdieck (1979), UTRC  
Report No. R79-954403-13, United Technologies Research  
Center, East Hartford, Connecticut.

D.H. France (1979), J. Inst. Energy 12, 169.

J.M. Harris, F.E. Lytle and T. C. McCain (1976), Anal. Chem.  
48, 2095.

B.S. Haynes, H. Jander and H. Gg. Wagner (1980), Ber.  
Bienseriges. Phys. Chem. 84, 585.

D.K. Killinger, C.C. Wang and M. Hanabusa (1976), Phys.

Rev. 13A, 2145.

R.P. Lucht (1979), M.S. Thesis, School of Mechanical  
Engineering, Purdue University, West Lafayette, Indiana.

R.P. Lucht and N.M. Laurendeau (1979), Appl. Opt. 18,  
856.

R.P. Lucht, D.W. Sweeney and N.M. Laurendeau (1979), DOE  
Progress Report C00-4939-1, School of Mechanical  
Engineering, Purdue University, West Lafayette, Indiana.

R.P. Lucht, D.W. Sweeney and N.M. Laurendeau (1980a), DOE  
Progress Report C00-4939-2, School of Mechanical  
Engineering, Purdue University, West Lafayette, Indiana.

R.P. Lucht, D.W. Sweeney and N.M. Laurendeau (1980a),  
Appl. Opt. 19, 3295.

R.P. Lucht, D.W. Sweeney and N.M. Laurendeau (1980c), in  
Laser Probes for Combustion Chemistry, ACS Symposium  
Series 134, D.R. Crosley, Ed., American Chemical  
Society, Washington, D.C.

T.J. McIlrath and J.L. Carlsten (1972), Phys. Rev. 6A,  
1091.

L. Pasternack, A.P. Baronavski and J.R. McDonald (1978),  
J. Chem. Phys. 69, 4830.

E.H. Piepmeier (1972a), Spectrochimica Acta 27B, 445.

C.C. Wang, D.K. Killinger and C.M. Huang (1980), Phys. Rev. 22A, 188.

A. Yariv (1975), Quantum Electronics, John Wiley and Sons, New York.